ARTICLE

Understanding the Effect of the Exchange-Correlation Functionals on Methane and Ethane Formation over Ruthenium Catalysts†

Chen Chen‡, Minzhen Jian‡, Jin-Xun Liu*, Wei-Xue Li*

Department of Chemical Physics, School of Chemistry and Materials Science, University of Science and Technology of China, Hefei 230026, China

(Dated: Received on March 25, 2022; Accepted on April 18, 2022)

Density functional theory (DFT) has been established as a powerful research tool for heterogeneous catalysis research in obtaining key thermodynamic and/or kinetic parameters like adsorption energies, enthalpies of reaction, activation barriers, and rate constants. Understanding of density functional exchange-correlation approximations is essential to reveal the mechanism and performance of a catalyst. In the present work, we reported the influence of six exchange-correlation density functionals, including PBE, RPBE, BEEF+vdW, optB86b+vdW, SCAN, and SCAN+rVV10, on the adsorption energies, reaction energies and activation barriers of carbon hydrogenation and carbon-carbon couplings during the formation of methane and ethane over Ru(0001) and Ru(10$\bar{1}$1) surfaces. We found the calculated reaction energies are strongly dependent on exchange-correlation density functionals due to the difference in coordination number between reactants and products on surfaces. The deviation of the calculated elementary reaction energies can be accumulated to a large value for chemical reaction involving multiple steps and vary considerably with different exchange-correlation density functionals calculations. The different exchange-correlation density functionals are found to influence considerably the selectivity of Ru(0001) surface for methane, ethylene, and ethane formation determined by the adsorption energies of intermediates involved. However, the influence on the barriers of the elementary surface reactions and the structural sensitivity of Ru(0001) and Ru(10$\bar{1}$1) are modest. Our work highlights the limitation of exchange-correlation density functionals on computational catalysis and the importance of choosing a proper exchange-correlation density functional in correctly evaluating the activity and selectivity of a catalyst.

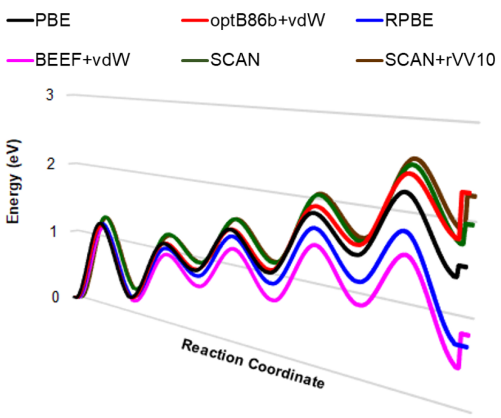

Key words: Density functional exchange-correlation approximation, Adsorption energy, Reaction energy, Activation barriers, Structural sensitivity

I. INTRODUCTION

Density functional theory (DFT) has become a standard tool for modeling heterogeneous catalysis in providing the atomic-scale understanding of the reaction mechanism and predicting the activity and selectivity of a catalyst by microkinetic simulations based

†Part of Special Topic "the 1st Young Scientist Symposium on Computational Catalysis".
‡These authors contributed equally to the work.
*Authors to whom correspondence should be addressed. E-mail: jxliu86@ustc.edu.cn, wxli70@ustc.edu.cn

on the calculated energetics [1, 2]. The formalism of DFT is exact with all the complexity hidden in the exchange-correlation functionals which holds the key to the success and the failure of DFT calculations [3]. Many semi-empirical parameters were used to simplify the exchange-correlation functionals as a function of electron density in DFT. Generally, the exchange-correlation functions based on density functional approximations were often constructed by fitting their parameters to benchmark data sets or formulated by satisfying appropriate constrains while fitting to appropriate norms [4]. Although DFT has been applied extensively to the investigation of heterogeneous catalysis, its application might suffer from large errors in predicting the thermodynamic and kinetic properties of chemical reactions [5–9] due to the deficiency of exchange-correlation approximations [10–12]. Therefore, much effort has been made to find the best density functional approximations, such as PBE [13], revPBE [14], RPBE [15], B3LYP [16], vdW-DF [17], DFT-D4 [18], SCAN [19] , HSE06 [20], to describe chemical reactions occurring at the surfaces and/or interfaces of solid materials.

In the past decades, DFT calculations with a wide variety of exchange-correlation density functionals were performed to calculate the heat of formation in gas [21–23], bond dissociation enthalpy [24], reaction barriers for gas phase reaction [25], solid-state properties [26–28] and adsorption of molecules on metal surfaces [29–35] in comparison with experimental measurements and/or high-level calculations. Many works indicate that different exchange-correlation density functionals can yield highly different surface properties of transition metal surfaces and adsorption energies. For example, PBE is the most widely used for surface chemistry studies [13], but it often underestimates the surface energies and work functions of transition metals surfaces [36]. RPBE can predict adsorption energies accurately on transition metal surfaces, but underestimate the surface energies of transition metals [37]. The optB86b-vdW, the non-empirical van-der-Waals density functional correction methods, can give better agreement with experimental estimation for CO_2 adsorption on Cu(111) as compared with PBE [38]. SCAN belonging to meta-GGA exchange-correlation density functional can achieve remarkable accuracy calculations for diversely bonded molecules and materials [19, 26, 39, 40], but it has a relative higher computational costs than GGA-type exchange-correlation density functionals. As is well-known, the catalytic activity and selectivity of a catalyst is determined by the adsorption strength of adsorbants/intermediates and activation barriers of chemical reactions on it. A variation of only 0.20 eV in barrier can result in an uncertainty of 2 orders of magnitude for the reaction rate at 500 K [5]. Therefore, it is highly desirable to find which exchange-correlation density functional is a good choice for accurate energetics calculations for a given heterogeneous catalytic system.

Fischer-Tropsch synthesis (FTS), which converts syngas into liquid fuels and chemicals, has attracted extensive attention due to the global depleting resources of crude oil [41–43]. The overall reaction paths of FTS procedure includes CO activation, hydrogenation of C_xH_y intermediates, hydrocarbons coupling and termination pathways [44]. Ruthenium (Ru) is a promising catalyst for FTS because of its higher activity and selectivity for CO conversion into long-chain hydrocarbon products as compared with Co- and Fe-based catalyst [45, 46]. The competition between the bond breaking and formation processes determines the activity and selectivity of FTS over Ru catalyst. Therefore, an adequate choice of exchange-correlation density functionals for DFT calculations is critical to accurately describe the covalent bonds in the gaseous molecule, the electronic/geometric structures of catalyst surface and the interactions between them because of the diversified problems caused by the delocalization of popular exchange-correlation density functionals. To the best of our knowledge, whether the errors of available exchange-correlation density functionals can be cancelled during mechanistic studies of methane and ethane formation involved in FTS over Ru catalyst remains an open question.

In the present work, DFT calculations were performed to compute the adsorption energies of C_xH_y intermediates, reaction energies and activation barriers of methane and ethane formation over Ru(0001) and Ru(10$\bar{1}$1) surfaces by adopting six different exchange-correlation density functionals, namely PBE, RPBE, BEEF+vdW, optB86b+vdW, SCAN and SCAN+rVV10. The two Ru(0001) and Ru(10$\bar{1}$1) surfaces selected here are based on their large surface areas exposure in the Wulff shape of Ru with hexagonal close-packed (HCP) crystal structure [47, 48]. We found the adsorption energies of C_xH_y intermediates and reaction energies of C_xH_y hydrogenation and C−C coupling reaction steps are highly dependent on exchange-

DOI:10.1063/1674-0068/cjcp2203049

correlation density functionals. The deviation in the calculated reaction energies is found to accumulate considerably for the reactions involving the multiple step and vary with exchange-correlation density functionals used. However, the different choice of exchange-correlation density functionals does not have a great influence on the energetics difference between different Ru(0001) and Ru(10$\bar{1}$1) surfaces. Our work provides a deep insight into the exchange-correlation density functionals effect on surface reactions, which advances our understanding of the limitations of the existing exchange-correlation density functionals.

II. CALCULATION METHODS

All periodic DFT calculations were performed using Vienna *ab initio* Simulation Package (VASP) [49, 50]. The Kohn-Sham equations were solved by using a plane-wave basis set [51] with a kinetic energy cutoff of 400 eV. The convergence criteria for electronic self-consistent interaction is specified by 10^{-4} eV. The ionic positions were relaxed until the residual average forces were less than 0.02 eV/Å. Transition states were determined by CI-NEB [52, 53] and improved dimer methods [54], and then verified to have one imaginary frequency lying along the reaction path. Six different exchange-correlation density functionals, namely, generalized-gradient approximation (GGA) functional PBE [13] and RPBE [15], non-local description of correlation optB86b+vdW [17] and BEEF+vdW [55], meta-GGA functional SCAN [19] and combine SCAN functional with long-range vdW interaction from rVV10:SCAN+rVV10 [56], were adopted to calculate the adsorption energies of C_xH_y intermediates, reaction energies and activation barriers of C_xH_y hydrogenation and C−C coupling for methane and ethane formation over Ru(0001) and Ru(10$\bar{1}$1) surfaces. DFT-GGA-PBE calculations were first performed to optimize the lattice constant of HCP Ru in the bulk phase, C_xH_y intermediates adsorption configurations and transition states involved in methane and ethane formation over Ru(0001) and Ru(10$\bar{1}$1) surfaces. Afterward, the geometric structure of adsorbed Ru surfaces was fixed for the single-point energy calculations using the other exchange-correlation density functionals. The lattice and adsorbates relaxation calculation results are nearly the same as the single point energy calculations with the variation of all the adsorption energies, reaction energies and activation barriers less than 0.20 eV among different exchange-correlation density functionals calculations (Table S1−S3 in Supplementary materials (SM)). Therefore, the single point energy calculations not only save computing resources, but also facilitate the analysis of the source of deviation between different exchange-correlation density functionals.

HCP Ru(0001) and Ru(10$\bar{1}$1) surfaces were modeled by a four-atomic-layers slab model with a (2×2) unit cell. A (6×6×1) k-point mesh was used to sample the surface Brillouin zone, and a 15 Å vacuum layer was introduced between the repeated slabs along the z-direction. During the surface structure optimization, the bottom two layers of the slabs were fixed at the bulk positions and the remaining Ru metal atoms and adsorbates were allowed to relax. The adsorption energies ($E_{\rm ads}$) of gas molecules can be calculated as the change in energy when a molecule is adsorbed on a solid surface:

$$E_{\rm ads} = E_{\rm slab\text{-}m} - E_{\rm slab} - E_{\rm m} \tag{1}$$

where $E_{\rm slab\text{-}m}$ and $E_{\rm slab}$ refer to the total energy of a surface with and without the adsorbate m. $E_{\rm m}$ is to the total energy of molecules or radicals in the gas phase. The reaction energy of an elementary reaction can be calculated as the energy difference of initial and final states:

$$\Delta E = E_{\rm slab\text{-}p} + E_{\rm slab} - E_{\rm slab\text{-}a} - E_{\rm slab\text{-}b} \tag{2}$$

where $E_{\rm slab\text{-}p}$, $E_{\rm slab\text{-}a}$, and $E_{\rm slab\text{-}b}$ are the total energies of products, reactant a and reactant b adsorbed on Ru(0001) and Ru(10$\bar{1}$1) surface, respectively. $E_{\rm slab}$ denotes the total energy of clean Ru(0001) and Ru(10$\bar{1}$1) surface.

Mean deviation (MD), mean absolute deviation (MAD) and mean absolute percent deviation (MAPD) were used to describe statistical energies difference between PBE and other exchange-correlation density functionals calculations:

$$\mathrm{MD} = \frac{\sum \text{values of DRV}}{\text{Total number of items}} \tag{3}$$

$$\mathrm{MAD} = \frac{\sum \text{absolute values of DRV}}{\text{Total number of items}} \tag{4}$$

$$\mathrm{MAPD} = \frac{\mathrm{MAD}}{\text{Mean value calculated by PBE}} \tag{5}$$

where DRV is the deviation from reference value.

DOI:10.1063/1674-0068/cjcp2203049

III. RESULTS AND DISCUSSION

A. C_xH_y adsorption on Ru(0001)

The adsorption of C_xH_y intermediates involved in methane and ethane formation over Ru(0001) surface was studied by DFT calculations using the six different exchange-correlation density functionals. Although the adsorption configurations and adsorption energies of C_xH_y intermediates on Ru(0001) surface are sensitive to the choice of exchange-correlation density functionals [57–61], we only considered exchange-correlation density functionals effect with C_xH_y intermediates adsorption at the most favorable sites determined by GGA-PBE calculations in the present work. The most widely used PBE functional was chosen as a reference to compare with other five exchange-correlation density functionals.

The optimized adsorption configurations of C_xH_y (x=0−2, y=0−6) intermediates involved in methane and ethane formation over Ru(0001) surface are shown in FIG. 1. C_xH_y intermediates prefer to adsorb at the fcc or hcp hollow sites over Ru(0001) surface. All the 16 intermediates can be divided into three categories according to coordination number (N_c) of intermediates bonded with metal, namely, type I: the intermediates physisorption on Ru surface with N_c of zero, type II: the intermediates chemisorption on Ru surface with N_c between 0 and 3 ($0<N_c\leq3$), type III: two C atoms in C_xH_y intermediates binding Ru surface strongly with N_c higher than 3. The adsorption energies of C_xH_y intermediates calculated by five different exchange-correlation density functionals with respect to PBE functional calculations are shown in FIG. 2(a, b). Obviously, the adsorption energies of C_xH_y intermediates are sensitive to the choice of exchange-correlation density functionals. As compared with PBE, optB86b+vdW significantly overestimates the adsorption strength of all C_xH_y intermediates on Ru(0001) surface, whereas RPBE often underestimates C_xH_y intermediates adsorption strength; BEEF+vdW calculations overestimate the adsorption of physisorbed system (CH_4 and CH_3CH_3) but underestimate that of chemisorbed systems. Our calculations are consistent with previous work that the adsorption energies predicted by BEEF+vdW calculations are always between those computed by PBE and RPBE calculations for the catalytic systems where vdW interaction contributes large amount to the adsorption energies [29]. The

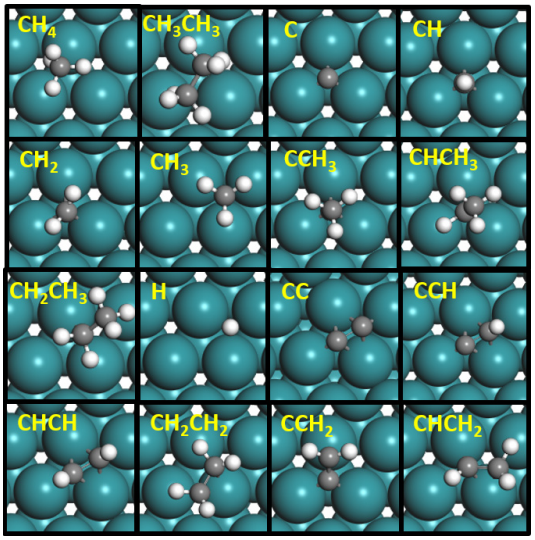

FIG. 1 The top view of C_xH_y intermediates adsorption configurations over Ru(0001) surface. Cyan, gray and white spheres are Ru, C, and H atoms, respectively. This notation is used throughout this work.

meta-GGA SCAN generally overestimates the adsorption strengths of all the adsorbents except for CH_x and $CHCH_3$ intermediates. Additionally, SCAN+rVV10 with the addition of long-range vdW interaction on the basis of SCAN overestimates the adsorption strengths of all types of C_xH_y intermediates.

The calculated adsorption strengths of C_xH_y intermediates over Ru(0001) change from strong to weak in the order of optB86b+vdW>SCAN+rVV10> SCAN>PBE>BEEF+vdW>RPBE. The deviations of the average adsorption energies of all the intermediates by different exchange-correlation density functionals are given in the term of MD, MAD, and MAPD as shown in FIG. 2(c). The absolute deviation MAD is calculated to vary from 0.12 eV to 0.43 eV for the statistical energy difference calculated by PBE and other five different exchange-correlation density functionals. Whereas the relative deviation (MAPD) is with much small change from 4% to 13% among different exchange-correlation density functionals.

The MAD of absolute adsorption energies calculated by the five different exchange-correlation density functionals referred to PBE is independent of the adsorption strength and the intermediates (FIG. 2(a, b)), but it is correlated well with the N_c of intermediates to Ru(0001) (FIG. 2(d) and Table S4 in SM). The larger variation of N_c for methyl adsorption on Ru(0001) surface can result in a larger MAD of adsorption energies difference

DOI:10.1063/1674-0068/cjcp2203049

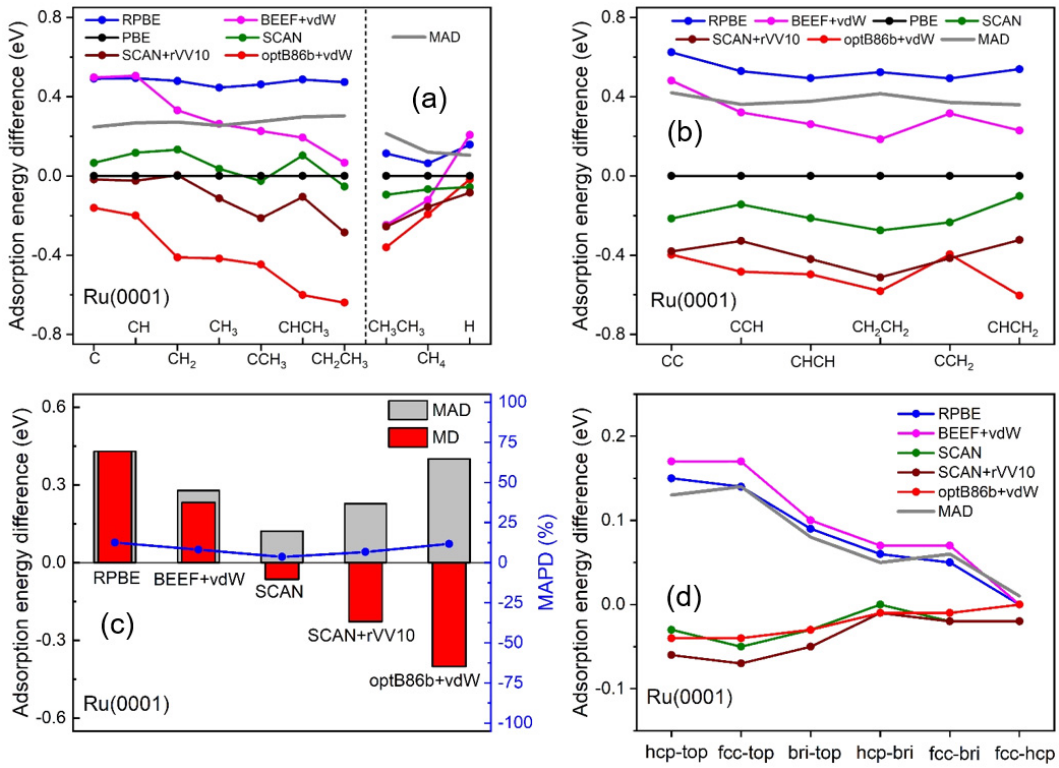

FIG. 2 The adsorption energies of C_xH_y intermediates calculated by various exchange-correlation density functionals with respect to PBE (a, b). (c) Statistical MD, MAD, and MAPD of the energy difference between PBE and other exchange-correlation density functionals calculations for C_xH_y intermediates adsorption on Ru(0001) surface. (d) The relationship between the adsorption energy difference and coordination number change for CH_3 adsorption over Ru(0001) by different exchange-correlation density functionals calculations. The hcp, fcc, bridge, top indicate CH_3 adsorption sites over Ru(0001) surface with a N_c of 3, 3, 2, and 1, respectively.

among different exchange-correlation density functionals calculations. Specifically, methyl (CH_3) adsorption energy varies significantly when the N_c transfers from 3 at hcp/fcc hollow sites to 1 at the top sites over Ru(0001), giving a large MAD by different exchange-correlation density functionals calculations. However, the adsorption energies do not change when methyl adsorption sites shift from hcp-hollow site to fcc-hollow site, showing a small MAD. The differences in adsorption energies among different exchange-correlation density functionals can be mainly attributed to the different N_c for the adsorption of intermediates.

B. Surface elementary reaction energies on Ru(0001)

The catalytic mechanism of methane, ethylene, and ethane formation over Ru(0001) surface was studied by six different exchange-correlation density functionals. The CH−CH coupling pathway, which was reported as the optimal route for long-chain growth [44, 62], was selected as the initial step for the formation of C_2 hydrocarbon species in the kinetic study. The calculated potential energy surfaces and corresponding transition states for methane, ethylene and ethane formation over Ru(0001) are shown in FIG. 3(a, b) and Table S5−S6 in SM. We find the reaction energies of all elementary steps involved in methane, ethylene and ethane formation are sensitive to the choice of exchange-correlation density functionals.

The calculated reaction energy of every elementary reaction is always underestimated or overestimated by different exchange-correlation density functionals calculations as compared with PBE calculation results, which results in an accumulation of small reaction energy deviations into a large one for the whole reaction cycles in methane, ethylene and ethane formation over Ru(0001) surface (FIG. 3(a, b)). The hydrogenation of CH intermediate towards methane is less endothermic by 0.69 eV for RPBE and BEEF+vdW calculations, but more than 1.85 eV endothermic for the other four PBE, optB86b+vdW, SCAN, and SCAN+rVV10 cal-

DOI:10.1063/1674-0068/cjcp2203049

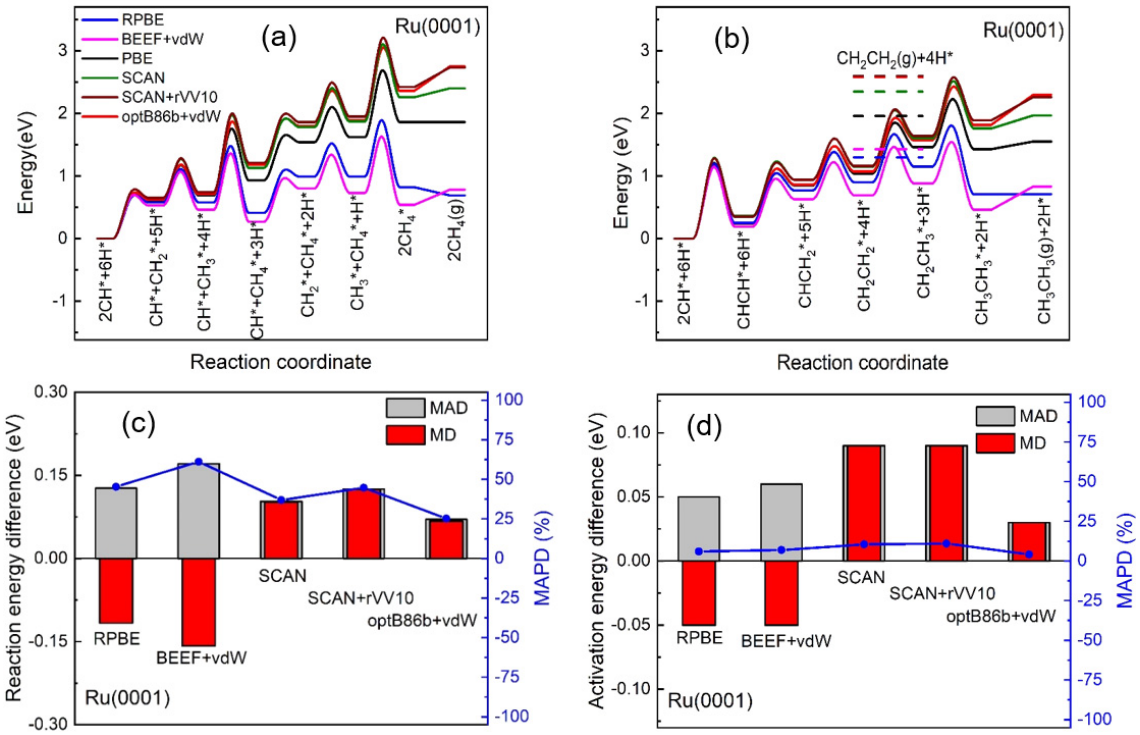

FIG. 3 Potential energy surfaces of (a) methane and (b) ethane formation over Ru(0001) by different exchange-correlation density functionals calculations. The dotted line indicates gaseous ethylene molecules formation energies. Statistical MD, MAD and MAPD of (c) all reaction energies and (d) activation energies by different exchange-correlation density functionals calculations referred to PBE calculation results.

culations. The same phenomenon can be also found for ethylene and ethane formation over Ru(0001) surface by six different exchange-correlation density functionals calculations. As a result, the apparent activation barrier for methane formation is nearly the same or higher than that of ethylene/ethane formation, which indicates a lower selectivity of methane than long-chain hydrocarbons in FTS [47, 63]. Whereas the selectivity of ethylene and ethane in C_2 products can be determined by the difference in desorption and hydrogenation activation barrier of ethylene in FIG. 3(b). We found PBE, optB86b+vdW, SCAN, and SCAN+rVV10 calculations show that the ethylene tends to be hydrogenated into ethane rather than desorption. In contrast, RPBE and BEEF+vdW calculations show a higher selectivity of ethylene than ethane, due to their predicted weakly adsorption strength of ethylene on Ru(0001) surface. Therefore, the selectivity of a chemical reaction is sensitive to the choice of exchange-correlation density functionals and it is crucial to choose a proper exchange-correlation density functional to predict the selectivity of a chemical reaction.

To understand the difference in the overall reaction energies of methane and ethane formation over Ru(0001) surface calculated by different exchange-correlation density functionals, we compared the reaction energies of each elementary steps (Table S7 in SM). We found the hydrogenation of CH_3* and CH_3CH_2* always has the largest contributions to the total deviations of reaction energies for methane and ethane formation by at least 40%, respectively, regardless of the used exchange-correlation density functionals. CH_3* and CH_3CH_2* intermediates chemisorb strongly while the formed CH_4* and CH_3CH_3* physisorb weakly on Ru(0001) surface with the coordination number change from 3 and 1 to 0, which results in great variations in the reaction energies calculated by different exchange-correlation density functionals (Table S8 in SM).

The calculated reaction energy differences between PBE and the other five exchange-correlation density functionals for methane and ethane formation (FIG. 3(c) and Table S9 in SM) indicate that all of 25 different surface elementary reactions have the same variation trend in reaction energy calculations for a given exchange-correlation density functional. Specifically, RPBE and BEEF+vdW calculations show lower

DOI:10.1063/1674-0068/cjcp2203049

reaction energies as compared with PBE calculations with the statistical MD of −0.12 and −0.16 eV, respectively. However, the reaction energies calculated by other three SCAN, SCAN+rVV10, and optB86b+vdw functionals have a positive MD less than 0.13 eV indicating an underestimation of reaction energy calculations as compared with PBE. The MAPD of calculated reaction energies varies larger than 25.19% for all different exchange-correlation density functionals, which indicates the choice of exchange-correlation density functionals has a serious impact on the reaction kinetics. The same conclusion can be found for activation barriers calculations by different exchange-correlation density functionals (FIG. 3(d) and Table S10−S11 in SM). The predicted MAPD is lower than 24.10%, demonstrating the less sensitivity of activation barriers calculations by using different exchange-correlation density functionals. However, more experimental measurements are needed to find the most favorable exchange-correlation density functionals to describe the surface chemical reactions qualitatively and quantitatively.

C. Sensitivity of exchange-correlation density functionals calculations on Ru(0001) and Ru(10$\bar{1}$1) surfaces

As is well known, the catalytic performance is determined by the geometric and electronic structures of the catalyst [64, 65]. Many works reported that the performance of FTS is strongly sensitive to the surface structures of Ru-based catalyst [47, 66–69]. To reveal the influence of exchange-correlation density functionals on the structure sensitivity of Ru catalyst, we studied the catalytic mechanism of methane and ethylene formation on Ru(0001) and Ru(10$\bar{1}$1) surfaces. The Ru(10$\bar{1}$1) surface selected here is based on its low surface energy and high exposure surface ratio in the Wulff shape of HCP Ru [47, 48]. The derivation trends in the calculated adsorption energies, reaction energies and activation barriers for methane and ethane formation on Ru(10$\bar{1}$1) surface are the same as Ru(0001) surface by different exchange-correlation density functionals calculations (FIG. S1−S3 and Table S12 in SM) where SCAN+rVV10 overestimates the reaction energies for almost all elementary reactions while the BEEF+vdW underestimates those on Ru(10$\bar{1}$1) most severely.

PBE calculations show the different adsorption and reaction energies for methane and ethane formation over Ru(0001) and Ru(10$\bar{1}$1) surfaces implying the structure sensitivity of Ru catalyst. The difference in the adsorption and reaction energies calculated by different exchange-correlation density functionals between the two Ru(0001) and Ru(10$\bar{1}$1) surfaces is almost the same as those calculated by PBE functional. Most difference in the adsorption and reaction energies calculations by different exchange-correlation density functionals between the two Ru(0001) and Ru(10$\bar{1}$1) surfaces is less than 0.04 eV (FIG. 4(a, b) and FIG. S4 in SM). Therefore, the different selection of exchange-correlation density functionals can describe the structure sensitivity of Ru(0001) and Ru(10$\bar{1}$1) surfaces well.

It is worth noting that there are still some points, which are the adsorption energies of unsaturated C, CH, and CCH_3 intermediates, derivating from the linear scaling relationship in FIG. 4(a). The reason can be attributed to the great changes in the coordination environment of these intermediates adsorption on the two different Ru(0001) and Ru(10$\bar{1}$1) surfaces. Specifically, the N_c of these three intermediates are three and four on Ru(0001) and Ru(10$\bar{1}$1), respectively, whereas the N_c of the remaining intermediates on the two surface is the same. Additionally, the deviated points can also be observed for reaction energies calculations of $C^*+C^*=CC^*+^*$, $C^*+H^*=CH^*+^*$, and $CCH_3{}^*+H^*=CHCH_3{}^*$ with great change in N_c for the intermediates adsorption before and after reaction on Ru(0001) and Ru(10$\bar{1}$1) surfaces in FIG. 4(b). Our work clearly reveal that the greater the change of coordination environment before and after the process, the greater deviation of the adsorption and reaction energies among various exchange-correlation density functionals calculations.

The statistical MD, MAD, and MAPD of the adsorption energies by different exchange-correlation density functionals calculations ranges from −0.05 eV to 0.08 eV, from 0.02 eV to 0.08 eV, and from 6.01% to 25.45%, respectively (FIG. 4(c) and Table S13 in SM), which further demonstrates the weak sensitivity of adsorption energies on different Ru surfaces even adopting different kinds of exchange-correlation density functionals. The MAD of surface reaction energy varies from 0.03 eV to 0.06 eV with the MAPD value below 14.17%, whereas the MAD becomes less than 0.05 eV with the MAPD below 21% for activation barriers calculations between Ru(0001) and Ru(10$\bar{1}$1) surfaces by different exchange-correlation density functionals (FIG. 4(d) and Table S14−S15 in SM). Therefore, the deviation of surface reaction energies and activation barriers is always

DOI:10.1063/1674-0068/cjcp2203049

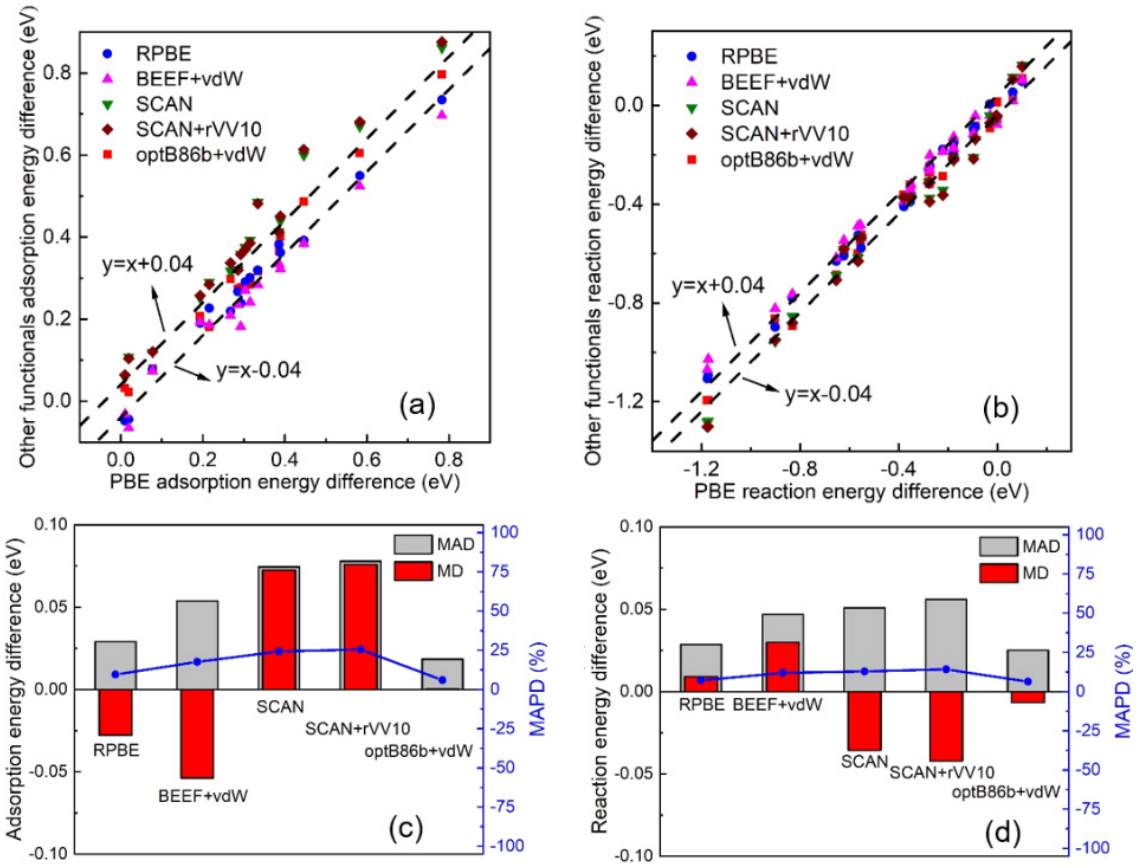

FIG. 4 The difference in the calculated (a) adsorption energy and (b) reaction energies between Ru(0001) and Ru(10$\bar{1}$1) surfaces by various exchange-correlation density functionals referred to PBE calculation results. Statistical MD, MAD and MAPD of (c) the adsorption energy and (d) reaction energy difference between Ru(0001) and Ru(10$\bar{1}$1) surfaces by different exchange-correlation density functionals calculations.

smaller than that of adsorption energies by adopting different exchange-correlation density functionals calculations. The differences of the calculated adsorption energies, reaction energies and activation energies among different surfaces are nearly constant for a given exchange-correlation density functional that identification of the energetic difference between two catalysts is independent of the choice of exchange-correlation density functionals while the investigation of the selectivity of a catalyst is exchange-correlation density functionals dependent.

IV. CONCLUSION

DFT calculations were performed to study the influence of exchange-correlation density functionals on the hydrogenation and carbon-carbon couplings in the formation of methane and ethane on Ru(0001) and Ru(10$\bar{1}$1) surfaces. We found the adsorption energies of 16 intermediates involved are sensitive to the exchange-correlation density functionals including PBE, RPBE, BEEF+vdW, optB86b+vdW, SCAN, and SCAN+rVV10. The large deviations of adsorption and reaction energies among different exchange-correlation density functionals are found from the coordination number change between reactants and products on the surfaces. The derivations can be accumulated for a chemical reaction containing multiple elementary reaction steps by different exchange-correlation density functionals calculations, which may affect significantly thermodynamics and even result in different selectivity of a chemical reaction. The reaction energies and activation barriers on metal surfaces are less sensitive to the exchange-correlation density functionals as compared with adsorption energies. Different exchange-correlation density functionals do not have a great influence on the investigation of the structural sensitivity. Our work highlights the limitation of diverse exchange-correlation density functionals in the computational

DOI:10.1063/1674-0068/cjcp2203049

catalysis and the importance of exchange-correlation density functionals in properly describing the energetics of a chemical reaction.

Supplementary materials: The optimized configurations, energy difference analysis diagrams, potential energy surfaces, calculated energetics, and statistical results are available.

V. ACKNOWLEDGMENTS

This work was supported by the Key Technologies R&D Program of China (No.2018YFA0208603), the National Natural Science Foundation of China (No.22172150 and No.91945302), the Chinese Academy of Sciences Key Project (QYZDJ-SSW-SLH054), the Start-up Funds of University of Science and Technology of China (No.KY2060000171), the National Natural Science Foundation of Anhui province (No.2108085QB62), USTC Research Funds of the Double First-Class Initiative (No.YD2060002012), K. C. Wong Education (No.GJTD-2020-15) and high-Performance Computational Resources provided by the University of Science and Technology of China (http://scc.ustc.edu.cn) and Hefei Advanced Computing center.

[1] J. K. Nørskov, F. Studt, F. Abild-Pedersen, and T. Bligaard, John Wiley & Sons, (2014).
[2] R. A. Van Santen, M. Neurock, and S. G. Shetty, Chem. Rev. **110**, 2005 (2009).
[3] A. J. Cohen, P. Mori-Sánchez, and W. Yang, Science **321**, 792 (2008).
[4] N. Q. Su and X. Xu, Annu. Rev. Phys. Chem. **68**, 155 (2017).
[5] E. Walker, S. C. Ammal, G. A. Terejanu, and A. Heyden, J. Phys. Chem. C **120**, 10328 (2016).
[6] H. Prats, P. Gamallo, R. Sayos, and F. Illas, Phys. Chem. Chem. Phys. **18**, 2792 (2016).
[7] J. P. McClure, O. Borodin, M. Olguin, D. Chu, and P. S. Fedkiw, J. Phys. Chem. C **120**, 28545 (2016).
[8] G. N. Simm and M. Reiher, J. Chem. Theory Comput. **12**, 2762 (2016).
[9] P. P. Chen, B. Y. Zhang, X. K. Gu, and W. X. Li, Chin. J. Chem. Phys. **32**, 437 (2019).
[10] M. Korth, Angew. Chem. Int. Ed. **56**, 5396 (2017).
[11] M. G. Medvedev, I. S. Bushmarinov, J. Sun, J. P. Perdew, and K. A. Lyssenko, Science **355**, 49 (2017).
[12] S. Hammes-Schiffer, Science **355**, 28 (2017).
[13] J. P. Perdew, K. Burke, and M. Ernzerhof, Phys. Rev. Lett. **77**, 3865 (1996).
[14] Y. Zhang and W. Yang, Phys. Rev. Lett. **80**, 890 (1998).
[15] B. Hammer, L. B. Hansen, and J. K. Nørskov, Phys. Rev. B **59**, 7413 (1999).
[16] P. J. Stephens, F. J. Devlin, C. F. Chabalowski, and M. J. Frisch, J. Phys. Chem. **98**, 11623 (1994).
[17] J. Klimeš, D. R. Bowler, and A. Michaelides, Phys. Rev. B **83**, 195131 (2011).
[18] E. Caldeweyher, S. Ehlert, A. Hansen, H. Neugebauer, S. Spicher, C. Bannwarth, and S. Grimme, J. Chem. Phys. **150**, 154122 (2019).
[19] J. Sun, A. Ruzsinszky, and J. P. Perdew, Phys. Rev. Lett. **115**, 036402 (2015).
[20] A. V. Krukau, O. A. Vydrov, A. F. Izmaylov, and G. E. Scuseria, J. Chem. Phys. **125**, 224106 (2006).
[21] B. T. Teng, X. D. Wen, M. Fan, F. M. Wu, and Y. Zhang, Phys. Chem. Chem. Phys. **16**, 18563 (2014).
[22] I. Y. Zhang and X. Xu, ChemPhysChem **13**, 1486 (2012).
[23] L. A. Curtiss, P. C. Redfern, and K. Raghavachari, J. Chem. Phys. **123**, 124107 (2005).
[24] J. Wu and X. Xu, J. Chem. Phys. **129**, 164103 (2008).
[25] L. Simon and J. M. Goodman, Org. Biomol. Chem. **9**, 689 (2011).
[26] Y. Zhang, D. A. Kitchaev, J. Yang, T. Chen, S. T. Dacek, R. A. Sarmiento-Pérez, M. A. L. Marques, H. Peng, G. Ceder, J. P. Perdew, and J. Sun, NPJ Comput. Mater. **4**, 1 (2018).
[27] Y. Meng, X. W. Liu, C. F. Huo, W. P. Guo, D. B. Cao, Q. Peng, A. Dearden, X. Gonze, Y. Yang, J. Wang, H. Jiao, Y. Li, and X. D. Wen, J. Chem. Theory Comput. **12**, 5132 (2016).
[28] P. Janthon, S. A. Luo, S.M. Kozlov, F. Vines, J. Limtrakul, D. G. Truhlar, and F. Illas, J. Chem. Theory Comput. **10**, 3832 (2014).
[29] C. T. Campbell, Surf. Sci. **640**, 36 (2015).
[30] F. Göltl, E. A. Murray, S. A. Tacey, S. Rangarajan, and M. Mavrikakis, Surf. Sci. **700**, (2020).
[31] P. Lazić, M. Alaei, N. Atodiresei, V. Caciuc, R. Brako, and S. Blügel, Phys. Rev. B **81**, 045401 (2010).
[32] S. Gautier, S. N. Steinmann, C. Michel, P. Fleurat-Lessard, and P. Sautet, Phys. Chem. Chem. Phys. **17**, 28921 (2015).
[33] P. S. Schmidt and K. S. Thygesen, J. Phys. Chem. C **122**, 4381 (2018).
[34] A. Stroppa, K. Termentzidis, J. Paier, G. Kresse, and J. Hafner, Phys. Rev. B **76**, 195440 (2007).
[35] S. J. Carey, W. Zhao, A. Frehner, C. T. Campbell, and B. Jackson, ACS Catal. **7**, 1286 (2017).
[36] A. Patra, J. E. Bates, J. Sun, and J. P. Perdew, Proc. Natl. Acad. Sci. USA **114**, E9188 (2017).
[37] A. Stroppa and G. Kresse, New J. Phys. **10**, 063020 (2008).

DOI:10.1063/1674-0068/cjcp2203049

[38] F. Muttaqien, Y. Hamamoto, I. Hamada, K. Inagaki, Y. Shiozawa, K. Mukai, T. Koitaya, S. Yoshimoto, J. Yoshinobu, and Y. Morikawa, J. Chem. Phys. **147**, 094702 (2017).
[39] F. Tran, J. Stelzl, and P. Blaha, J. Chem. Phys. **144**, 204120 (2016).
[40] J. Sun, R. C. Remsing, Y. Zhang, Z. Sun, A. Ruzsinszky, H. Peng, Z. Yang, A. Paul, U. Waghmare, and X. Wu, Nat. Chem. **8**, 831 (2016).
[41] A. Y. Khodakov, W. Chu, and P. Fongarland, Chem. Rev. **107**, 1692 (2007).
[42] Y. P. Pei, J. X. Liu, Y. H. Zhao, Y. J. Ding, T. Liu, W. D. Dong, H. J. Zhu, H. Y. Su, L. Yan, J. L. Li, and W. X. Li, ACS Catal. **5**, 3620 (2015).
[43] H. Wang, W. Zhou, J. X. Liu, R. Si, G. Sun, M. Q. Zhong, H. Y. Su, H. B. Zhao, J. A. Rodriguez, S. J. Pennycook, J. C. Idrobo, W. X. Li, Y. Kou, and D. Ma, J. Am. Chem. Soc. **135**, 4149 (2013).
[44] I. A. W. Filot, R. A. van Santen, and E. J. M. Hensen, Catal. Sci. Technol. **4**, 3129 (2014).
[45] T. Koh, H. M. Koo, T. Yu, B. Lim, and J. W. Bae, ACS Catal. **4**, 1054 (2014).
[46] J. M. G. Carballo, J. Yang, A. Holmen, S. García-Rodríguez, S. Rojas, M. Ojeda, and J. L. G. Fierro, J. Catal. **284**, 102 (2011).
[47] W. Z. Li, J. X. Liu, J. Gu, W. Zhou, S. Y. Yao, R. Si, Y. Guo, H. Y. Su, C. H. Yan, W. X. Li, Y. W. Zhang, and D. Ma, J. Am. Chem. Soc. **139**, 2267 (2017).
[48] H. Lin, J. X. Liu, H. Fan, and W. X. Li, J. Phys. Chem. C **124**, 11005 (2020).
[49] G. Kresse and J. Furthmüller, Phys. Rev. B **54**, 11169 (1996).
[50] G. Kresse and J. Furthmüller, Comput. Mater. Sci. **6**, 15 (1996).
[51] G. Kresse and D. Joubert, Phys. Rev. B **59**, 1758 (1999).
[52] G. Henkelman and H. Jónsson, J. Chem. Phys. **113**, 9978 (2000).
[53] G. Henkelman, B. P. Uberuaga, and H. Jónsson, J. Chem. Phys. **113**, 9901 (2000).
[54] J. Kastner and P. Sherwood, J. Chem. Phys. **128**, 014106 (2008).
[55] J. Wellendorff, K. T. Lundgaard, A. Møgelhøj, V. Petzold, D. D. Landis, J. K. Nørskov, T. Bligaard, and K. W. Jacobsen, Phys. Rev. B **85**, 235149 (2012).
[56] H. Peng, Z. H. Yang, J. P. Perdew, and J. Sun, Phys. Rev. X **6**, 041005 (2016).
[57] P. J. Feibelman, B. Hammer, J. K. Nørskov, F. Wagner, M. Scheffler, R. Stumpf, R. Watwe, and J. Dumesic, J. Phys. Chem. B **105**, 4018 (2001).
[58] J. C. Rodriguez-Reyes, C. G. Siler, W. Liu, A. Tkatchenko, C. M. Friend, and R. J. Madix, J. Am. Chem. Soc. **136**, 13333 (2014).
[59] S. Karakalos, Y. Xu, F. Cheenicode Kabeer, W. Chen, J.C. Rodriguez-Reyes, A. Tkatchenko, E. Kaxiras, R. J. Madix, and C. M. Friend, J. Am. Chem. Soc. **138**, 15243 (2016).
[60] M. Gajdo, A. Eichler, and J. Hafner, J. Phys.: Condens. Matter **16**, 1141 (2004).
[61] T. L. M. Pham, D. V. N. Vo, H. N. T. Nguyen, and N. N. Pham-Tran, Appl. Surf. Sci. **481**, 1327 (2019).
[62] Z. P. Liu and P. Hu, J. Am. Chem. Soc. **124**, 11568 (2002).
[63] D. Liuzzi, F. J. Pérez-Alonso, and S. Rojas, Fuel **293**, 120435 (2021).
[64] R. A. Van Santen, Acc. Chem. Res. **42**, 57 (2009).
[65] L. Liu and A. Corma, Chem. Rev. **118**, 4981 (2018).
[66] S. Shetty, A. P. Jansen, and R. A. van Santen, J. Am. Chem. Soc. **131**, 12874 (2009).
[67] S. Shetty and R. A. van Santen, Catal. Today **171**, 168 (2011).
[68] B. T. Loveless, C. Buda, M. Neurock, and E. Iglesia, J. Am. Chem. Soc. **135**, 6107 (2013).
[69] X. Y. Quek, I. A. Filot, R. Pestman, R. A. van Santen, V. Petkov, and E. J. Hensen, Chem. Commun. (Camb.) **50**, 6005 (2014).

DOI:10.1063/1674-0068/cjcp2203049